Phys. Status Solidi B **252**, No. 4, 683–688 (2015) / **DOI** 10.1002/pssb.201451444

physica status solidi b
www.pss-b.com
basic solid state physics

High-pressure effects on the intersubband optical absorption coefficient and relative refractive index change in an asymmetric double δ-doped GaAs quantum well

K. A. Rodríguez-Magdaleno[1,2], J. C. Martínez-Orozco[*,2,3], I. Rodríguez-Vargas[2], M. E. Mora-Ramos[1], and C. A. Duque[3]

[1] Facultad de Ciencias, Universidad Autónoma del Estado de Morels, Av. Universidad 1001, CP 62209, Cuernavaca, Morelos, México
[2] Unidad Académica de Física, Universidad Autónoma de Zacatecas, Calzada Solidaridad esquina con Paseo la Bufa S/N, C.P. 98060, Zacatecas, Zac., México
[3] Grupo de Materia Condensada-UdeA, Instituto de Física, Facultad de Ciencias Exactas y Naturales, Universidad de Antioquia UdeA, Calle 70 No. 52-21, Medellín, Colombia

Received 26 August 2014, revised 10 February 2015, accepted 2 March 2015
Published online 26 March 2015

Keywords absorption coefficient, δ-doping, high pressure, refractive index

* Corresponding author: e-mail jcmover@fisica.uaz.edu.mx, Phone: +52 492 9256690, Fax: +52 492 9241314

In the framework of the effective mass approximation and using a Thomas–Fermi-like model for the conduction band potential energy profile, the effects of hydrostatic pressure on the linear and nonlinear intersubband optical response of an asymmetric double δ-doped quantum well are studied. In particular, the intersubband coefficients of light absorption and the relative refractive index change in the system were calculated. It is found that the pressure causes a redshift of the signal response as well as a reduction in the coefficients's amplitudes. We have also found that the asymmetry of the potential profile clearly affects the relative refractive index change because, as long as the system becomes more asymmetric, this physical property becomes diminished.

1 Introduction The δ-doped profile is an important quantum confined system both from the fundamental and the practical points of view. Actually, the δ-doping concept is related to an impurity seeding profile – ideally, in a single atomic layer of the host material – and not to the potential energy function by itself. Wood et al. [1] made emphasis on the superiority of the molecular beam epitaxy method over other well known semiconductor growth technics, and introduced the concept of the atomic plane doping. The atomic plane doping profile was implemented in a field effect transistor by Schubert et al. [2, 3]. They named this system a δ-FET. This kind of doping profile was soon implemented in other important semiconductor structures as δ-doped superlattices and was demonstrated, from Shubnikov–de Hass oscillation experiments, that the single δ-doped quantum well exhibits two-dimension subbands in a V-shaped quantum well [4]. The first theoretical study in the Thomas–Fermi approximation for a single δ-doped impurities seeding was put forward by Ioriatti in 1990 [5]. He deduced an analytical self-consistent expression for the potential profile within the one-dimensional local-density approximation that resembles a V-shaped potential quantum well. After that, this potential profile has been implemented, for instance, in the theoretical determination of the subband energy level structure of n- and p-type double δ-doped quantum wells [6, 7] and in transport properties in double n-type δ-doped quantum wells in Silicon [8]. And more recently, in intersubband optical properties as a function of electric field [9].

The electronic structure and the interband and intersubband optical properties as well as other physical properties of interest for coupled double or multiple quantum wells are very active research fields [10–17]. In particular, the double

δ-doped quantum well is also a subject of great interest [9, 18–21] because its doping profile allows to modulate the band bending for the valence and conduction bands as a function of the impurities density. The double δ-doped system has potential applications in far infrared photodetectors because the intersubband absorption coefficient resonant peaks are in this range of the electromagnetic spectrum. It must be mentioned that this kind of doping profile has been also implemented as a source of charge carriers for semiconductor heterostructures [17, 22].

In this work, we are interested in investigating the effects produced by the hydrostatic pressure not only on the electronic structure of a double δ-doped system but also on the linear and nonlinear intersubband optical absorption and relative refractive index change coefficients. For that, we follow the Thomas–Fermi approximation, worked out by Ioriatti in the high-density limit [5]. In this context there exist some previous works. For instance, some years ago the energy level structure of a single δ-doped quantum well was reported as a function of the hydrostatic pressure considering the Γ–X crossover that occurs in GaAs when pressure goes beyond 13 kbar [23]. There are also studies of the effect of hydrostatic pressure on the excitonic spectrum of single δ-doped systems [24] and in the optical and transport properties for δ-doped structures [25–27]. It is well known that the Fermi level is pinned by surface states as reported in references [28, 29] and it depends, for metal–semiconductor contacts, of the presence of metal-induced gap states (MIGS). But in the present work, we are considering the Fermi level located between the ground and the first excited state of the δ-doped quantum well electronic structure in order to be possible the main intersubband optical absorption.

The organization of the work is as follows: In Section 2, we briefly presents the description of the theoretical model. In Section 3, one finds the corresponding results and discussion. Then in Section 4, we write down the main conclusions of our study.

2 Theoretical framework In this work, we investigate the optical absorption coefficient and the relative refraction index change related to intersubband energy transitions in an asymmetric double δ-doped quantum well. In the Thomas–Fermi approximation, a potential profile for the double δ-doped quantum well was proposed in previous work [9]. Using effective atomic units (Bohr radius and Rydberg) it is given by

$$V(z) = -\frac{\alpha^2}{(\alpha\left|z - l_p/2\right| + z_0^l)^4} - \frac{\alpha^2}{(\alpha\left|z + l_p/2\right| + z_0^r)^4}, \tag{1}$$

where $\pm l_p/2$ represents the distance, measured from the origin, for the left- and right-hand δ-doped impurities layers, respectively; $\alpha = 2/15\,\pi$, and

$$z_0^{l,r} = \left(\frac{\alpha^3}{\pi\, N_{2d}^{l,r}}\right)^{1/5}. \tag{2}$$

In the last expression $N_{2d}^{l,r}$ represents the density of ionized impurities for the left-hand (right-hand) side δ-doped layer.

As mentioned, in this work we consider the effect of hydrostatic pressure (P) on the system through the dependency of the electron effective mass $m_e^*(P)$ [30]:

$$\frac{m_e^*(P)}{m_0} = \left[1 + \frac{15\,020}{1519 + 10.7P} + \frac{7510}{1519 + 10.7P + 341}\right]^{-1}, \tag{3}$$

with m_0 the free electron mass. On the other hand, the static dielectric constant as a function of the hydrostatic pressure $\varepsilon_r(P)$ is measured experimentally by Samara [31] and is given by

$$\varepsilon_r(P) = 12.82\ \exp\left[-1.67 \times 10^{-3} P\right]. \tag{4}$$

In this work, we also take into account the change in system's dimensions due to the hydrostatic pressure. It is included through the size parameters as reported by Lefebvre et al. [32]:

$$l_p(P) = l_p(0)\left[1 - (S_{11} + 2S_{12})P\right]. \tag{5}$$

Here $S_{11} = 1.16 \times 10^{-3}\,\text{kbar}^{-1}$ and $S_{12} = -3.7 \times 10^{-4}$ kbar^{-1} are the GaAs elastic compliance constants. Besides, $l_p(0)$ represents the zero applied pressure length. Since the potential in our system is completely determined by the two-dimensional impurity densities, the only parameter that is affected by this compression is the distance between δ-doped sheets l_p.

Then, the Hamiltonian for the confined electron motion is given by

$$H = \left[-\frac{\hbar^2}{2\,m_e^*(P)}\frac{d^2}{dz^2} + V(z, P)\right], \tag{6}$$

where the confining potential, $V(z, P)$, is given by Eq. (1) (see Fig. 1). This differential equation is solved by means of a diagonalization procedure, based in the expansion of the wave function $\psi_m(z)$ in terms of the complete set of sinusoidal solutions of an infinite rectangular potential well of width L_∞ (which is assumed much larger than the other involved distances in the structure):

$$\psi_m(z) = \sum_{m=1}^{\infty} c_m \sqrt{\frac{2}{L_\infty}} \sin\left[\frac{m\pi}{L_\infty} z + \frac{m\pi}{2}\right]. \tag{7}$$

Of course, from the numerical point of view, it is not possible to consider an infinite set of base functions, so in this computation we extend the summation until $m = 50$. This base size ensures a good level of convergence and, as

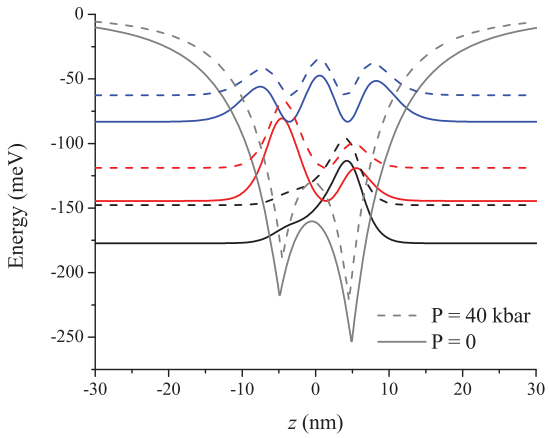

Figure 1 Potential profile and probability densities for the ground state (black line), first excited (red line), and second excited (blue line) states for zero hydrostatic pressure (solid line) and $P = 40$ kbar (dashed line). The ionized impurity density for the left-hand side δ-doped sheet is $N_{2d}^{l} = 5.0 \times 10^{12}\,\mathrm{cm}^{-2}$, while the right-hand side impurity sheet density is $N_{2d}^{r} = 6.5 \times 10^{12}\,\mathrm{cm}^{-2}$. The separation distance between δ-doped layers is $l_p(0) = 9.8$ nm.

shown in Ref. [9], the obtained electronic structure is in good agreement with a previous self-consistent computation.

With respect to the intersubband transition optical properties, it is reported by Ahn and Chuang [33] and by Takagahara [34] that for enough small values of the incident light intensity (I) it is possible to use a procedure for solving the Von Neumann's equation for the density matrix $\hat{\rho}$ in terms of a multi-order expansion. This allows to obtain expressions for the first and third order intersubband optical absorption coefficients, which are given by

$$\alpha^{(1)}(\omega) = \omega\, e^2 \sqrt{\frac{\mu_0}{\varepsilon_0 \varepsilon_r}} \left[\frac{\rho \hbar \Gamma_{10} |M_{10}|^2}{(E_{10} - \hbar\omega)^2 + (\hbar\Gamma_{10})^2} \right] \tag{8}$$

and

$$\alpha^{(3)}(\omega) = -\sqrt{\frac{\mu_0}{\varepsilon_0 \varepsilon_r}} \left(\frac{\omega\, e^4\, I}{2 n_r \varepsilon_0 c} \right) \times \frac{\rho\, \hbar \Gamma_{10} |M_{10}|^2}{[(E_{10} - \hbar\omega)^2 + (\hbar\Gamma_{10})^2]^2} \left\{ 4|M_{10}|^2 - \frac{|M_{11} - M_{00}|^2 [3E_{10}^2 - 4E_{10}\hbar\omega + \hbar^2(\omega^2 - \Gamma_{10}^2)]}{E_{10}^2 + (\hbar\Gamma_{10})^2} \right\}. \tag{9}$$

So, the total absorption coefficient is

$$\alpha^{(T)}(\omega) = \alpha^{(1)}(\omega) + \alpha^{(3)}(\omega)\,. \tag{10}$$

On the other hand, we can write down the expressions for the linear contribution to the relative change in the refractive index:

$$\frac{\Delta n^{(1)}(\omega)}{n_r} = \frac{e^2\, \rho\, |M_{10}|^2}{2\, n_r^2\, \varepsilon_0} \frac{E_{10} - \hbar\,\omega}{(E_{10} - \hbar\,\omega)^2 + (\hbar\,\Gamma_{10})^2}, \tag{11}$$

meanwhile the third order correction is given by

$$\frac{\Delta n^{(3)}(\omega)}{n_r} = -\frac{|M_{10}|^2}{4 n_r^3 \varepsilon_0} \frac{e^4\, \rho\, \mu_0\, c\, I}{[(E_{10} - \hbar\omega)^2 + (\hbar\Gamma_{10})^2]^2} \times \left[4(E_{10} - \hbar\omega)|M_{10}|^2 - \frac{(M_{11} - M_{00})^2}{(E_{10})^2 + (\hbar\Gamma_{10})^2} \times \left\{ (E_{10} - \hbar\omega)[E_{10}(E_{10} - \hbar\omega) - (\hbar\Gamma_{10})^2] - (\hbar\Gamma_{10})^2 (2E_{10} - \hbar\omega) \right\} \right]. \tag{12}$$

The total relative change of the refractive index, $\Delta n(\omega)/n_r$, is the sum of these two contributions. In these expressions, $E_{10} = E_1 - E_0$ is the transition energy difference between allowed intersubband transitions, e is the elementary charge, μ_0 is the magnetic permeability of vacuum, ε_0 is the free-space dielectric permittivity, and c is the speed of light in vacuum. Γ_{10} is the associated damping rate, $\rho = (\rho_{ii} - \rho_{ff})/S$ is the 2D density of carriers involved in the transition (ρ_{jj} being the equilibrium thermal occupation number of the j-th state), and $n_r = \sqrt{\varepsilon_r}$ is the refractive index of the material in the active region of the structure.

3 Results and discussion We present the theoretical computation of the intersubband transition optical absorption and relative refractive index change coefficients for the asymmetric double δ-doped quantum well (ADDQW). For the sake of clarity, we go back to usual – nonatomic – units. The electronic level structure is calculated considering values of the hydrostatic pressure within the range of 0–40 kbar (1 kbar = 0.1 GPa). The separation distance between δ-doped layers is varied within the range of 5–15 nm, and its dependency on P is given by Eq. (5). The parameters related to the intersubband transition optical properties are: laser intensity $I = 0.1 \times 10^{10}\,\mathrm{W\,m^{-2}}$ and the relaxation transition time $T_{10} = 0.2 \times 10^{-12}\,\mathrm{s}$ ($\Gamma_{10} = 1/T_{10}$). The bulk carrier density, ρ, is assumed to be of about $3.8 \times 10^{22}\,\mathrm{m^{-3}}$, and the other parameters are well known physical quantities.

Figure 1 shows the potential profile of an ADDQW, considering $N_{2d}^{l} = 5.0 \times 10^{12}\,\mathrm{cm^{-2}}$ and $N_{2d}^{r} = 6.5 \times 10^{12}\,\mathrm{cm^{-2}}$, with inter-δ-layer distance $l_p = 9.8$ nm. The corresponding δ-doped potential minimum energies for the left-hand and right-hand side δ-doped QWs are −217 and −253 meV, respectively. By using dashed lines, we depict the energy levels in the system when this is under a hydrostatic pressure of 40 kbar. Due to the hydrostatic pressure effects the potential profile becomes narrower and less deeper than under zero pressure conditions. This potential profile deformation is mainly due to the pressure-induced variation of the effective mass (see Eq. (3)) and the static dielectric constant (see Eq. (4)). Besides, the influence of P on the value l_p is such that

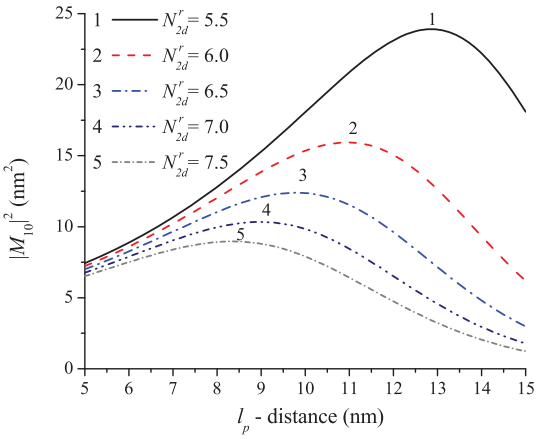

Figure 2 Square of main dipole matrix element $|M_{10}|^2$ as a function of the separation distance (l_p) between δ-doped sheets of impurities for five different values of the right-hand side sheet impurity density (N^r_{2d} in units of $\times 10^{12}$ cm^{-2}) while the left-hand side impurity density is fixed to $N^l_{2d} = 5.0 \times 10^{12}$ cm^{-2}.

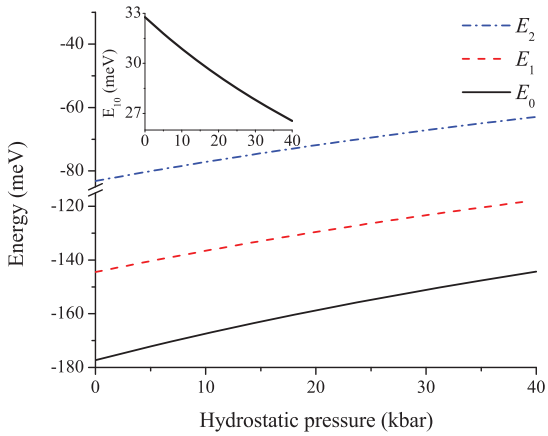

Figure 3 Energy levels for the ground (black solid line) and the first two excited states (colored dashed lines) as functions of the hydrostatic pressure in the range from zero to 40 kbar. In the inset appears the behavior of the main energy difference (E_{10}). The results are for $N^r_{2d} = 6.5 \times 10^{12}$ cm^{-2} and $l_p(0) = 9.8$ nm.

that, for a pressure value of 40 kbar, this distance diminishes in approximatively 2% ($l_p = 9.6$ nm). It is possible to notice that the ground and first excited state (represented by black and red lines, respectively) are clearly affected by the quantum well asymmetry, meanwhile the second excited state is not significantly modified.

In Fig. 2, we present the square of the main dipole matrix element ($|M_{10}|^2$) for a ADDQW as a function of the separation distance between δ-doped layers under zero hydrostatic pressure conditions. This computation allows us to investigate the separation distance between sheets, for each configuration, at which the dipole matrix element has a maximum. For this analysis, we have fixed the left-hand side ionized impurity density to $N^l_{2d} = 5.0 \times 10^{12}$ cm^{-2} and considered several values $N^r_{2d} = 5.5$, 6.0, 6.5, 7.0, and 7.5 in units of 10^{12} cm^{-2}. It can be observed that the corresponding maximum values of $|M_{10}|^2$ appear at distances of 12.9, 10.9, 9.8, 9.0 , and 8.4 nm, respectively. In principle, this enables us to propose a specific separation distance l_p in order to maximize the intersubband transition optical properties that we are interested in. In general, when the separation distance is small enough (about 5 nm), all the dipole matrix elements has almost the same magnitude $|M_{10}|^2 \approx 7$ nm^2 due to the small change of the spatial extension of the involved wavefunctions, disregarding the variation of the sheet density values. However, as the separation distance rises, this magnitude increases until it reaches the maximum – which becomes more prominent in the case of $N^r_{2d} = 5.5 \times 10^{12}$ cm^{-2} with a value of 22 nm^2. This happens because, as long as l_p augments, there is a configuration in which the overlap of the wavefunctions is optimum. But if one further increases this separating distance, the larger values of $|z|$ will lie on regions of opposite sign of the wavefunctions of the ground and first excited states – or over regions of almost zero values of them. This is confirmed by the above-mentioned situation of $N^r_{2d} = 5.5 \times 10^{12}$ cm^{-2}. For this concentration, the potential well profile is the most similar to a symmetric double δ-doped QW – with respect to the origin. By observing the positions of the corresponding maxima of those states in Fig. 1, one can realize about this phenomenon. For analogous arguments, as long as N^r_{2d} rises, this maximum value decreases just because each time the potential profile departs from symmetry.

Since the aim of this work is to study the effect of the hydrostatic pressure on the intersubband transition optical properties of interest, we choose the separation distance, that maximizes the square of the dipole matrix element $|M_{10}|^2$ and then, by means of Eqs. (3)–(5), we introduce the hydrostatic pressure effects. Figure 3 contains the energy level positions as functions of the hydrostatic pressure in the case of $N^r_{2d} = 6.5 \times 10^{12}$ cm^{-2} with $l_p(0) = 9.8$ nm. It is readily observed that the ground state (black solid line) monotonically increases due to hydrostatic pressure effects, and the same behavior can be seen for the excited states (dashed lines). Nevertheless the rate of increase for the ground state is higher than that of the first excited state (the effect of narrowing of the confining potential profile is more pronounced at the bottom), in such a way that the main energy difference (E_{10}) diminishes as a function of the hydrostatic pressure, as shown in the inset of Fig. 3. Therefore, it is possible to predict a redshift in the intersubband transition optical properties due to the hydrostatic pressure effect.

Now, as we already discussed above, the linear and third order contributions to the intersubband optical absorption and relative refractive index change coefficients directly depend on the square of the main energy transition dipole matrix element ($|M_{10}|^2$). On the other hand, the third order correction expressions contain a term that incorporates the asymmetry of the potential profile through the factor $|M_{11} - M_{00}|^2$, which actually represents an information about the permanent electric dipoles in the system, provided that in most occasions only the lowest energy subbands

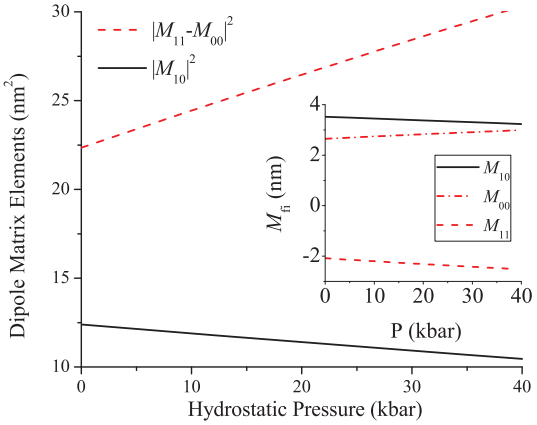

Figure 4 Main dipole matrix element $|M_{10}|^2$ (black solid line) and asymmetry factor $|M_{11} - M_{00}|^2$ (red dashed line) for an asymmetric double δ-doped quantum well as functions of the hydrostatic pressure. In the inset, we present the variations for the dipole matrix elements M_{00} – red dash-dotted line, M_{11} – red dashed line, and M_{10} – black solid line.

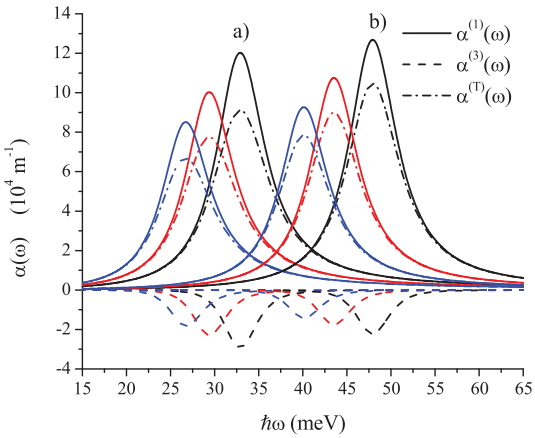

Figure 5 Intersubband absorption coefficient for an asymmetrical double δ-doped quantum well as a function of the incident photon energy and the hydrostatic pressure, for two different values of the right-hand side ionized impurity density. (a) $N^{r}_{2d} = 6.5 \times 10^{12}$ cm^{-2} with $l_p = 9.8$ nm. (b) $N^{r}_{2d} = 7.5 \times 10^{12}$ cm^{-2} with $l_p = 8.4$ nm. A fixed value of $N^{l}_{2d} = 5.0 \times 10^{12}$ cm^{-2} is taken in both cases. Black lines correspond to $P = 0$, the red lines are for $P = 20$ kbar, whereas the blue lines correspond to $P = 40$ kbar.

are occupied. Thus, we report these dipole moment matrix elements as functions of hydrostatic pressure in Fig. 4, in order to gain inside on the influence of the hydrostatic pressure and the asymmetry factor on the intersubband transition optical response. We can observe that the square of the main energy transition dipole matrix goes from a value of 12.4 nm^2 at zero pressure to a value of about 9 nm^2 at $P = 40$ kbar. This means that it decreases nearly 30% and this will, eventually, reflect on the optical properties due to intersubband transition. The permanent dipole factor ($|M_{11} - M_{00}|^2$) (red dashed line) has, for zero hydrostatic pressure conditions, a value of 22 nm^2. For finite increasing pressure, it monotonically augments until it reaches a value of 30 nm^2 for $P = 40$ kbar. This means that the hydrostatic pressure induces a higher degree of polarization, which may be related to a greater degree of asymmetry in the system. To clarify this situation in the inset of Fig. 4, we present the behavior of both $|M_{00}|$ and $|M_{11}|$. It is clearly observed that the magnitude of these two quantities increases as a result of the increment in the hydrostatic pressure and, given that they have opposite signs, the permanent dipole factor becomes larger, which justifies naming it as the "asymmetry factor."

In Fig. 5, we plot the linear $[\alpha^{(1)}(\omega)]$, third-order nonlinear $[\alpha^{(3)}(\omega)]$ and total intersubband absorption coefficients $[\alpha^{(T)}(\omega)]$ for our ADDQW. They are represented by solid, dashed and point-dashed lines, respectively. In obtaining this figure, we have considered two different system configurations that correspond to taking two different values of N^{r}_{2d}, and of the l_p associated with the maximum (at zero pressure) of $|M_{01}|$); keeping N^{l}_{2d} fixed. Three different values of P have been used as parameters: 0, 20, and 40 kbar (black, red, and blue lines, respectively).

The effect of applying a finite pressure on the system is detected, as it was predicted above, via a redshift of the resonant intersubband absorption peaks as well as a reduction of their amplitudes. On the other hand, going to a larger value of the right-hand impurity sheet density results in a blueshift of the optical response. This is particularly true within the range of N^{r}_{2d} above 5.5×10^{12} cm^{-2}, as it was shown in Ref. [9].

Finally, in Fig. 6, we show the coefficient of relative refractive index change due to intersubband transitions using the same set of parameters as in the previous Fig. 5. We may also notice here the redshift effect due to the application of hydrostatic pressure to the system, together with the blueshift associated with the increment in N^{r}_{2d}, as commented above. What is different in this case is the significant reduction in

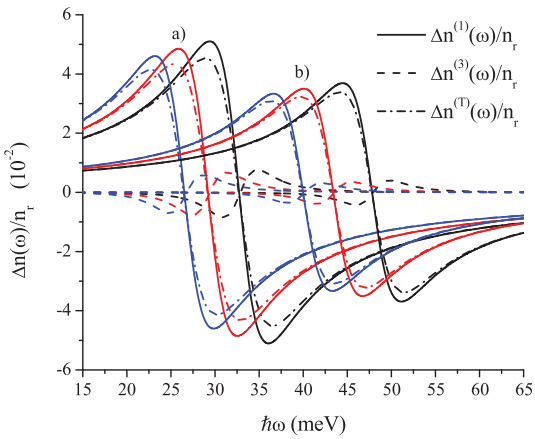

Figure 6 Relative refractive index change due to intersubband transitions for an asymmetrical double δ-doped quantum well as a function of incident photon energy and the hydrostatic pressure (P) for two different values of the right-hand side impurity density (N^{r}_{2d}); (a) 6.5×10^{12} cm^{-2} ($l_p = 9.8$ nm) and (b) 7.5×10^{12} cm^{-2} ($l_p = 8.4$ nm) and fixed left-hand side impurity density, $N^{l}_{2d} = 5.0 \times 10^{12}$ cm^{-2}. Pressure values are the same considered in Fig. 5.

the amplitude of this physical quantity when the impurities density augments. This fact can be explained having in mind that, in that case, the system becomes more asymmetrical, which is reflected in the decrease of the factor $|M_{10}|$ (see Fig. 2). By observing the expressions for the linear and nonlinear contributions to this coefficient, one realizes that their amplitudes are mainly governed by this factor, contrary to the case of $\alpha(\omega)$ where the resonant factor $\omega = \omega_{10} = E_{10}/\hbar$ predominates.

4 Conclusions In this paper, we have reported a study of the electronic structure as well as the intersubband related optical absorption and relative refractive index change coefficients for asymmetric double n-type δ-doped quantum wells in GaAs, under hydrostatic pressure effects. In general it can be concluded that the main effect of hydrostatic pressure, with respect to the optical properties due to intersubband transitions, is to induce a redshift of the resonant peaks and nodes, for the absorption coefficient and for the relative refraction index change, respectively, which are typically in the far infrared spectral region. It is also observed that the magnitude of the optical absorption resonant peaks decreases as the hydrostatic pressure rises, independently of the system's configuration. On the other hand, we have also found that the asymmetry of the potential profile clearly affects the relative refractive index change because, as long as the system becomes more asymmetric, the relative refractive index change coefficient becomes diminished.

Acknowledgements J.C.M.O. acknowledge to the Mexican National Council of Science and Technology (CONACyT) for support through its program Estancias Postdoctorales y Sabáticas al Extranjero para la consolidación de Grupos de Investigación with number 207848 and also to the Autonomous University of Zacatecas for its grant for this sabbatical stay. J.C.M.O. is also grateful to the Universidad de Antioquia for hospitality during his sabbatical stay. MEMR thanks Mexican CONACYT for support through research grant CB-2008-101777. C.A.D. is grateful to the Colombian Agencies CODI-Universidad de Antioquia (Estrategia de Sostenibilidad 2014–2015 de la Universidad de Antioquia), Facultad de Ciencias Exactas y Naturales-Universidad de Antioquia (CAD-exclusive dedication project 2014–2015), and El Patrimonio Autónomo Fondo Nacional de Financiamiento para la Ciencia, la Tecnología y la Innovación, Francisco José de Caldas.

References

[1] C. E. C. Wood, G. Metze, J. Berry, and L. F. Eastman, J. Appl. Phys. **51**, 383–387 (1980).
[2] E. F. Schubert and K. Ploog, Jpn. J. Appl. Phys. **24**, L608–L610 (1985).
[3] E. F. Schubert, A. Fischer, and K. Ploog, IEEE Trans. Electron Devices **33**, 625–632 (1986).
[4] K. Ploog, Phys. Scr. **1987**, 136 (1987).
[5] L. Ioriatti, Phys. Rev. B **41**, 8340–8344 (1990).
[6] I. Rodríguez-Vargas, L. M. Gaggero-Sager, and V. R. Velasco, Surf. Sci. **537**, 75–83 (2003).
[7] I. Rodríguez-Vargas and L. M. Gaggero-Sager, Rev. Mex. Fis. **50**, 614–619 (2004).
[8] I. Rodríguez-Vargas and L. M. Gaggero-Sager, J. Appl. Phys. **99**, 033702 (2006).
[9] K. A. Rodríguez-Magdaleno, J. C. Martínez-Orozco, I. Rodríguez-Vargas, M. E. Mora-Ramos, and C. A. Duque, J. Lumin. **147**, 77–84 (2014).
[10] H. F. Xu and N. Liu, Physica E **60**, 183–187 (2014).
[11] A. M. Schönhöbel, J. A. Girón-Sedas, and N. Porras-Montenegro, Physica B **442**, 74–80 (2014).
[12] W. X. Yang, J. W. Lu, Z. K. Zhou, L. Yang, and R. K. Lee, J. Appl. Phys. **115**, 203104 (2014).
[13] R. L. Restrepo, G. L. Miranda, C. A. Duque, and M. E. Mora-Ramos, J. Lumin. **131**, 1016–1021 (2011).
[14] F. Ungan, U. Yesilgul, S. Sakiroglu, E. Kasapoglu, H. Sari, and I. Sökmen, J. Lumin. **143**, 75–80 (2013).
[15] M. E. Mora-Ramos, C. A. Duque, E. Kasapoglu, H. Sari, and I. Sökmen, J. Lumin. **135**, 301–311 (2013).
[16] H. R. Hamedi, Physica B **440**, 83–87 (2014).
[17] T. Sahu, S. Palo, and A. K. Panda, J. Appl. Phys. **113**, 083704 (2013).
[18] D. J. Carter, O. Warschkow, N. A. Marks, and D. R. McKenzie, Phys. Rev. B **87**, 045204 (2013).
[19] S. Das, R. K. Nayak, T. Sahu, and A. K. Panda, J. Appl. Phys. **115**, 073701 (2014).
[20] J. G. Rojas-Briseño, J. C. Martínez-Orozco, I. Rodríguez-Vargas, M. E. Mora-Ramos, and C. A. Duque, Phys. Status Solidi B **251**(415–422) (2014).
[21] J. G. Rojas-Briseño, J. C. Martínez-Orozco, I. Rodríguez-Vargas, M. E. Mora-Ramos, and C. A. Duque, Physica B **424**, 13–19 (2013).
[22] V. Tulupenko, A. Abramov, Y. Belichenko, V. Akimov, T. Bogdanova, V. Poroshin, and O. Fomina, J. Appl. Phys. **109**, 064303 (2011).
[23] M. E. Mora-Ramos and C. A. Duque, Braz. J. Phys. **36**, 866–868 (2006).
[24] M. E. Mora-Ramos and C. A. Duque, Physica B **415**, 72–76 (2013).
[25] E. Ozturk and Y. Ozdemir, Opt. Commun. **294**, 361–367 (2013).
[26] O. Oubram, I. Rodríguez-Vargas, and J. C. Martínez-Orozco, Rev. Mex. Fis. **60**, 161–167 (2014).
[27] O. Oubram, M. E. Mora-Ramos, and L. M. Gaggero-Sager, Eur. Phys. J. B **71**, 233–236 (2009).
[28] S. Ernst, A. Goñi, K. Syassen, and K. Eberl, Phys. Rev. Lett. **72**, 4029–4032 (1994).
[29] A. Goñi, S. Ernst, K. Syassen, and K. Eberl, J. Phys. Chem. Solids **56**(3–4), 367–373 (1995).
[30] N. Raigoza, A. L. Morales, A. Montes, N. Porras-Montenegro, and C. A. Duque, Phys. Rev. B **69**, 045323 (2004).
[31] G. Samara, Phys. Rev. B **27**, 3494–3505 (1983).
[32] P. Lefebvre, B. Gil, and H. Mathieu, Phys. Rev. B **35**, 5630–5634 (1987).
[33] D. Ahn and S. L. Chuang, IEEE J. Quantum Electron. **23**, 2196–2204 (1987).
[34] T. Takagahara, Phys. Rev. B **36**, 9293–9296 (1987).

